

NACA RM L55H11

62 63475
~~CONFIDENTIAL~~

Copy 340
RM L55H11

Declassified by authority of NASA
Classification Change Notices No. 181
Dated ** 8/15/69

X80K-04



RESEARCH MEMORANDUM

FLIGHT INVESTIGATION OF A ROLL-STABILIZED RAM-JET TEST
VEHICLE OVER A MACH NUMBER RANGE OF 2.3 TO 2.7

By Thomas L. Kennedy and Otto F. Trout, Jr.

Langley Aeronautical Laboratory
Langley Field, Va.

FF No. 602(D)	X69-76954	(THRU)
	(ACCESSION NUMBER)	
	<u>27</u>	<u>NONE</u>
	(PAGES)	(CODE)
	(NASA CR OR TMX OR AD NUMBER)	(CATEGORY)
AVAILABLE TO U.S. GOVERNMENT AGENCIES		

Restriction/Classification Cancelled

NATIONAL ADVISORY COMMITTEE FOR AERONAUTICS

WASHINGTON
October 7, 1955

~~CONFIDENTIAL~~

D E C L A S S I F I E D

NATIONAL ADVISORY COMMITTEE FOR AERONAUTICS

RESEARCH MEMORANDUM
Declassified by authority of NASA
Classification Change Notices No. 121
Dated ** 8/15/69FLIGHT INVESTIGATION OF A ROLL-STABILIZED RAM-JET TEST
VEHICLE OVER A MACH NUMBER RANGE OF 2.3 TO 2.7
By Thomas L. Kennedy and Otto F. Trout, Jr.


SUMMARY

A flight investigation has been conducted on a roll-stabilized ram-jet test vehicle. Engine performance data are presented over a Mach number range of 2.3 to 2.7, a range of fuel-air ratio of 0.038 to 0.050, and an altitude range of 3,000 to 40,000 feet. Roll-control performance is presented over a Mach number range of approximately 2.3 to 2.4. Theoretical values of the half amplitude and the period of the self-sustained roll oscillation show good agreement with experimental results.

INTRODUCTION

In recent years there has been an increasing interest in missiles capable of cruising at supersonic speeds. One method of flying other than a ballistic trajectory is to roll stabilize the missile and provide lift. Since a ram-jet powered missile could readily be used as a cruising missile, a flight test of a ram-jet test vehicle similar to those investigated in references 1 and 2 has been made with the addition of a flicker-type automatic roll-stabilization system having a displacement-plus-rate response.

Ram-jet performance was obtained in the Mach number range 2.3 to 2.7 and a fuel-air ratio range of 0.035 to 0.050. Roll-control system performance was obtained in the Mach number range 2.3 to 2.4 with a corresponding dynamic pressure range of 7,000 to 4,500 pounds per square foot. The ram-jet test vehicle was flight-tested at the Langley Pilotless Aircraft Research Station, Wallops Island, Va.





SYMBOLS

A_{ϕ}	half amplitude of the self-sustained roll oscillation (half total amplitude displacement), deg
b	wing span, ft
C_D	drag coefficient
C_{l_p}	roll-damping coefficient derivative
$C_{l_{\delta}}$	control-moment coefficient derivative
C_T	ram-jet thrust coefficient
C_{T_G}	gross thrust coefficient
C_{T_N}	net thrust coefficient
F	thrust, lb
F/A	weight fuel-air ratio
H_D	total pressure at the exit of the diffuser, lb/sq ft
H_O	free-stream total pressure, lb/sq ft
h	altitude, ft
I_x	moment of inertia of vehicle about longitudinal axis, slug-ft ²
M	Mach number
\dot{m}	fuel rate, lb/sec
P	period of the self-sustained roll oscillation, sec
p	free-stream static pressure, lb/sq in. abs
q	dynamic pressure, lb/sq ft
R	Reynolds number based on mean chord of delta wing

T	free-stream static temperature, °F abs
V	vehicle velocity, ft/sec
x	horizontal range, ft
δ	deflection angle of one aileron, deg
λ	gyro rate factor, radian/radian/sec
τ	time lag in operation of the ailerons, sec
$\dot{\phi}$	rolling velocity, deg/sec

MODEL DESCRIPTION

Airframe


Photographs presenting top and side views of the test vehicle are shown in figure 1. The principal dimensions and general arrangement of the test vehicle are shown in figure 2. The vehicle differs from the test vehicles reported in references 1 and 2 in that a 9-inch cylindrical section was added forward of the fuel tank to accommodate the roll-control gyros, and a 60° delta vertical fin with tip ailerons was used in place of the swept vertical fin.

The vehicle weighed 311 pounds including 25 pounds of fuel. The moment of inertia about the longitudinal axis of the vehicle was 2.1 slug feet squared.

Ram-Jet Engines

Two identical ram jets were used to power the vehicle. Figure 3 shows a sectional view of the engine and its component parts. The engines were constructed with aluminum cowls and inner bodies. The burners and combustion shells were of inconel with mild steel exit nozzles. The engines each had an inlet capture area of 0.085 square foot and a design Mach number of 2.1. The combustion-chamber design was identical to that used in references 1, 2, and 3. The exit nozzles had a throat to combustion-chamber area ratio of 0.853 and throat to exit area ratio of 0.826.

Burnout-type starting disks, similar to those described in reference 3, were used. Electric delay squibs ignited the engines during boost at a Mach number of about 1.6. A motorized needle valve was used



to regulate the fuel flow at a predetermined rate. The valve was also used to program the firing of the booster and ram-jet ignition. The fuel tank was charged with 25 pounds of commercial grade ethylene (C_2H_4) fuel at about 1,100 pounds per square inch.

Roll-Stabilization System

The roll autopilot, similar to that analyzed in reference 4, is classed as a flicker-type autopilot having a displacement-plus-rate response. The all-electrical components consisted of gyro unit, power relay, and solenoid-type servos. These components are shown in figure 4. In operation, displacement of the model in roll actuates the power relay through a commutator pickoff on the displacement gyro. The rate gyro provided lead by displacement of the commutator. Action of the power relay energizes the appropriate solenoid servo calling for corrective aileron displacement. The ailerons were linked together to provide equal simultaneous deflection of $\pm 3^\circ$ and were hinged at $66\frac{2}{3}$ percent of the aileron root chord. Maximum expected aileron aerodynamic hinge moment was estimated to be about 40 inch-pounds. The airframe-autopilot combination is characterized by an oscillatory flight condition, with the amplitude and frequency of the oscillations dependent upon airframe, autopilot, and aerodynamic parameters. The autopilot characteristics, as determined in laboratory tests, are given in table I. The aerodynamic parameters given in table II were obtained by using linear theory to extend the data of reference 4.

INSTRUMENTATION

Continuous-wave Doppler radar was used to measure the velocity of the test vehicle and an NACA modified SCR-584 radar was used to obtain the flight path. Atmospheric data were obtained from a radiosonde balloon released just prior to launching.

An NACA 10-channel telemeter transmitted continuous signals of free-stream pitot stagnation pressure (two ranges), longitudinal acceleration, aileron position, rate of roll, transverse acceleration, right engine diffuser-exit total pressure and combustion-chamber static pressure, left engine diffuser-exit total pressure, and fuel injection pressure.

FLIGHT TEST

Flight test of the vehicle was conducted at the Pilotless Aircraft Research Station at Wallops Island, Va. A photograph of the model

booster combination is shown in figure 5. The test vehicle was connected to the booster by a free-to-roll coupling. The vehicle was launched at a 75° elevation angle. The gyro power was applied remotely at -30 seconds (30 seconds prior to booster ignition), and uncaged remotely at -15 seconds. Vehicle fuel programmer power was applied remotely at 0.0 time, firing the booster at 1.3 seconds and igniting the ram-jet engines at 3.5 seconds at a Mach number of 1.6. The M5 missile booster accelerated the vehicle to a Mach number of 2.3 at a time of 4.6 seconds. The vehicle accelerated to a peak Mach number of 2.68 at 20.5 seconds when the left engine flamed out. The right engine continued to burn until approximately 25 seconds. The vehicle had decelerated to a Mach number of 2.4 when it was lost by Doppler radar.

At booster separation the vehicle was stable in roll and continued stable until 12.5 seconds. After 12.5 seconds the ailerons failed to respond and the model continued to roll for the duration of the flight at a roll velocity of about 500° per second.

ANALYSIS OF DATA AND DISCUSSION

Test Conditions

The flight path as obtained from SCR-584 radar with pertinent flight points indicated is shown in figure 6. The static temperature and pressure time history for the flight is shown in figure 7. The Mach number time history of the flight is shown in figure 8 and the Reynolds number time history of the flight based on the mean chord of the delta fin is shown in figure 9.

Engine Performance

The net thrust, defined as the actual net propulsive force, was determined from telemetered longitudinal acceleration and the vehicle mass corrected for fuel consumption. Net thrust coefficient, based on total engine area of both engines 0.462 square foot, is shown in figure 10. Also shown is the external drag coefficient obtained during vehicle coast and the external drag coefficient of reference 1. The drag coefficient of reference 1 was used to obtain gross thrust coefficient in the higher Mach number range since deceleration with one engine in operation precluded the determination of drag for this vehicle at the higher speeds. Even though the vehicles differed slightly in configuration, the drag coefficients appear to agree within experimental accuracy indicating that the drag coefficient of reference 1 is a good approximation for this vehicle.



The gross thrust coefficient based on engine cross-sectional area is shown in figure 11 as a function of Mach number. The thrust coefficient shown for one-engine operation is based on the area of both engines and is adjusted for the internal drag of the dead engine. The fuel-air ratios presented for 100-percent combustion efficiency obtained from the various values of gross thrust coefficient, Mach number, and free-stream temperature were determined by the method presented in reference 3. The actual fuel-air ratio was determined from fuel rates experienced in ground tests of the fuel system and calculated air rates from the flight test.

The gross thrust, and fuel rates obtained from ground tests, and those calculated for 100-percent combustion efficiency are shown in figure 12. No fuel rates are shown after burnout of the first engine since considerable error would be introduced in working with one engine in operation.

The total pressure recovery of the engines for the ram-jet portion of the flight is shown as a function of Mach number in figure 13. The diffuser-exit total pressure was measured by integrating rakes installed at the diffuser-exit and the free-stream total pressure was calculated from free-stream static pressure and Mach number. The recovery is considerably lower than the maximum possible due to engine operation at low thrust coefficient during free flight. The engines at all times were operating well below their maximum thrust coefficient and above design Mach number.

Roll Autopilot Performance

A sample of the aileron position and rolling velocity as they appeared on the telemeter record is shown in figure 14. By integrating the roll velocity record, the amplitude of the self-sustained roll oscillation was obtained. The period of the oscillation was obtained by measurement of the time for one complete cycle. Presented in figure 15 are the actual and theoretical period and amplitude of the roll oscillation as a function of dynamic pressure. The method presented in the appendix of reference 5 was used to calculate the theoretical curves shown in the figure. The theoretical amplitude and period were calculated for two conditions, one using the constant time lag τ determined in laboratory tests, and the other using the values of τ obtained from the flight test. Values of τ in the flight tests were obtained by measurement of the time required for the ailerons to go from start of reversal to half reversal and adding this increment to the time required from the initiation of signal to start of reversal as obtained in laboratory tests. Using the time lag obtained in flight, the theory shows good agreement with experimental data. Up to the time of 6.5 seconds the value of τ was constant and slightly higher than that experienced in



laboratory tests. This portion of the flight is represented in the figure by the dynamic pressure range from 6,900 to 6,000 lb/sq ft. After 6.5 seconds τ gradually increased with a corresponding increase in the amplitude and period as is shown in the figure for dynamic pressures less than 6,000 lb/sq ft.

After 12.5 seconds the ailerons remained against a stop, except for a slight movement every 180° of roll displacement, indicating that the gyro was signaling for opposite aileron. As the vehicle decelerated, it traversed the speed range through which the roll system had previously operated satisfactorily; however, there was no indication of aileron response in spite of the large decrease in dynamic pressures at the later times. The inability of the ailerons to respond at any time after 12.5 seconds over the wide range of conditions tends to indicate that an electrical or mechanical failure in the solenoid servo motor or aileron linkage was responsible for the roll system divergence.

CONCLUDING REMARKS

In the flight test of a roll-stabilized ram-jet test vehicle, the following points were observed:

1. The ram-jet engines operated satisfactorily over a Mach number range of 2.3 to 2.7 in free-flight at fuel-air ratios of 0.038 to 0.050 and over an altitude range of 3,000 to 40,000 feet.
2. The roll-control system operated satisfactorily during the initial part of the flight. Theoretical values of the half amplitude and period show good agreement with experimental results.

Langley Aeronautical Laboratory,
National Advisory Committee for Aeronautics,
Langley Field, Va., July 28, 1955.

REFERENCES

1. Faget, Maxime A., and Dettwyler, H. Rudolph: Initial Flight Investigation of a Twin-Engine Supersonic Ram Jet. NACA RM L50H10, 1950.
2. Dettwyler, H. Rudolph, and Bond, Aleck C.: Flight Performance of a Twin-Engine Supersonic Ram Jet From 2,300 to 67,200 Feet Altitude. NACA RM L50L27, 1951.
3. Faget, Maxime A., Watson, Raymond S., and Bartlett, Walter A., Jr.: Free-Jet Tests of a 6.5-Inch-Diameter Ram-Jet Engine at Mach Numbers of 1.81 and 2.00. NACA RM L50L06, 1951.
4. Zarovsky, Jacob, and Gardiner, Robert A.: Flight Investigation of a Roll-Stabilized Missile Configuration at Varying Angles of Attack at Mach Numbers Between 0.8 and 1.79. NACA RM L50H21, 1951.
5. Curfman, Howard J., Jr.: Theoretical Analysis of the Rolling Motions of Aircraft Using a Flicker-Type Automatic Roll Stabilization System Having a Displacement-Plus-Rate Response. NACA RM L8K23a, 1949.

TABLE I.- ROLL AUTOPILOT CHARACTERISTICS

Aileron deflection	$\pm 3^{\circ}$
Displacement gyro:	
Voltage, d-c	24
Speed, rpm	9,600
Rate gyro:	
Voltage, d-c	24
Speed, rmp	10,600
Rate factor, λ , radian/radian/sec	0.16
Solenoid servomotor:	
Voltage, d-c	24
Current amperes, d-c	9.6
Stroke, in.	0.14
Tractive force at 0.14 in.	
Stroke at 105° C, lb	31
Effective aileron lever arm, in.	1.33
Autopilot time lag, τ , sec	0.05

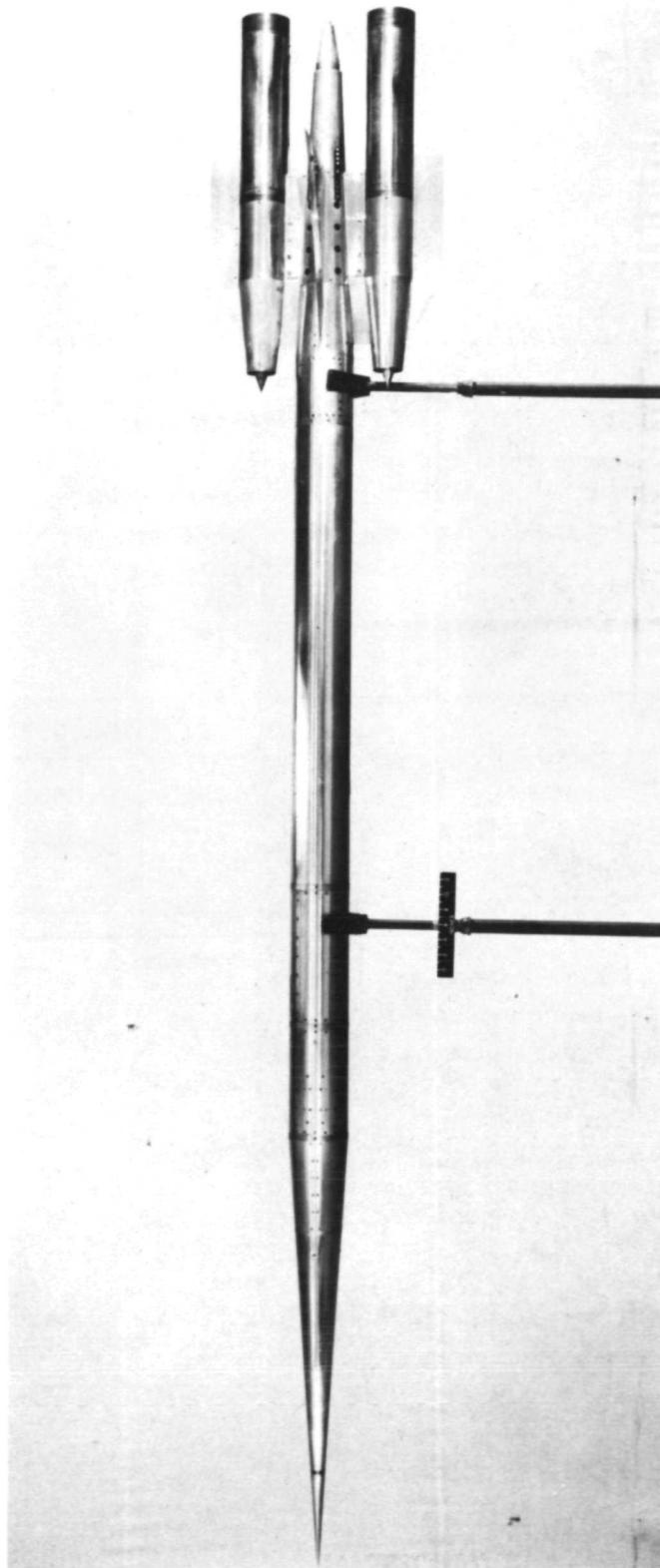
(From time signal originates in gyro to 1/2 throw of ailerons)

TABLE II.- AERODYNAMIC COEFFICIENTS USED TO OBTAIN
 AUTOPILOT THEORETICAL CURVES AND TIME LAG τ AS
 DETERMINED FROM THE FLIGHT

[Coefficients based on radian measure
 and wing area of 4.44 sq ft]

	M = 2.33	M = 2.37	M = 2.44
Control moment coefficient, $C_{l\delta}$	0.0368	0.0357	0.0340
Roll-damping coefficient, C_{lp}	-0.2115	-0.208	-0.202
Time lag, τ , sec	0.055	0.0575	0.082

DECLASSIFIED

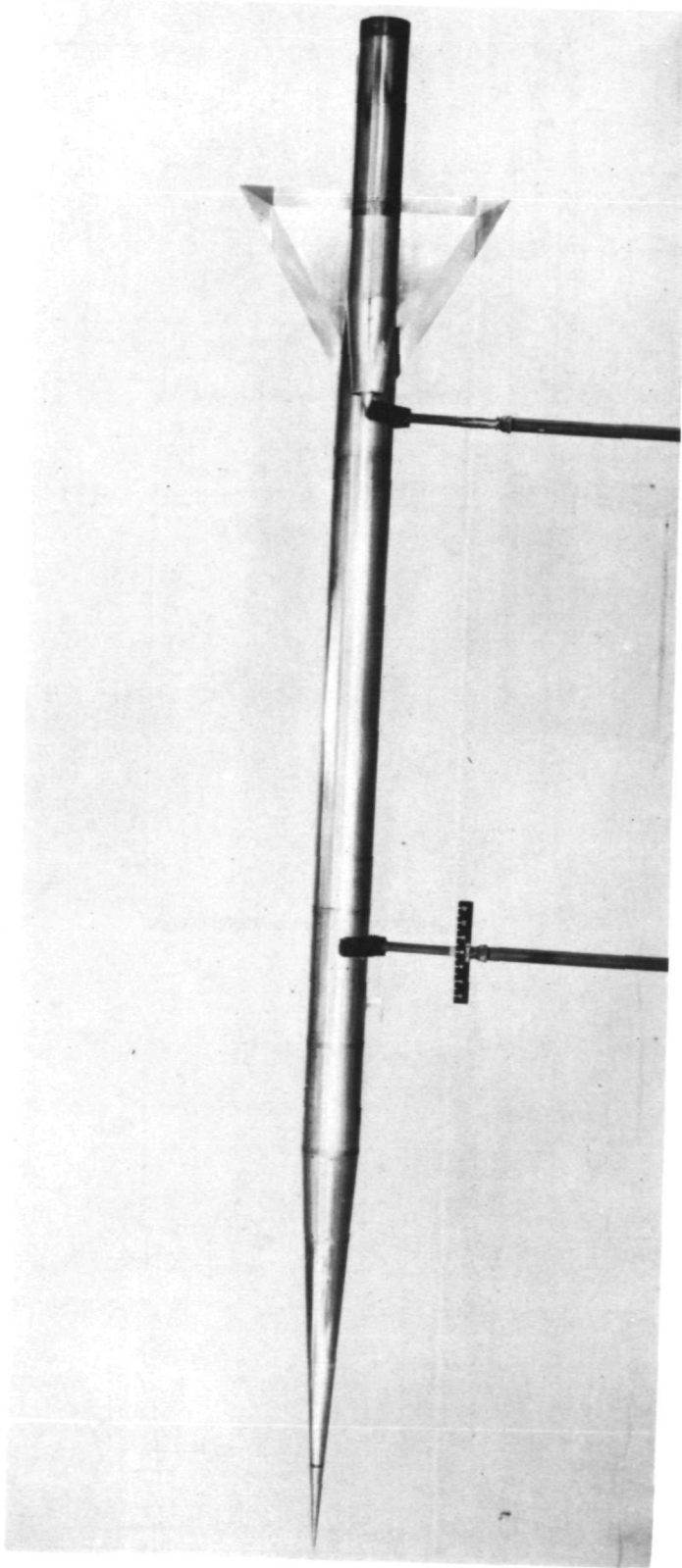


L-86134.1

(a) Showing ram-jet engines.

Figure 1.- Photograph of test vehicle.

CONFIDENTIAL



L-86133.1

(b) Showing vertical fins with tip ailerons.

Figure 1.- Concluded.

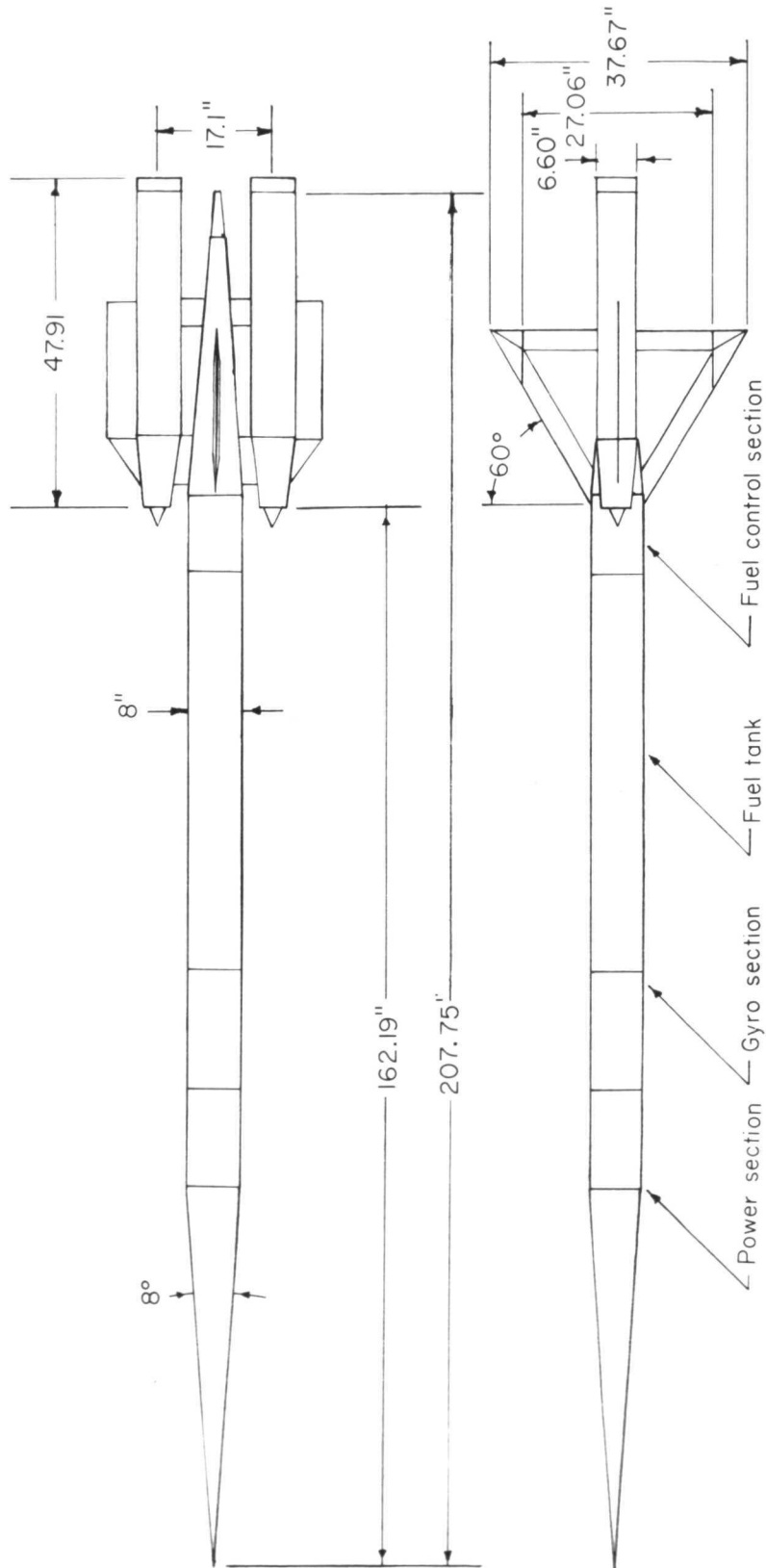


Figure 2.- Sketch of test vehicle.

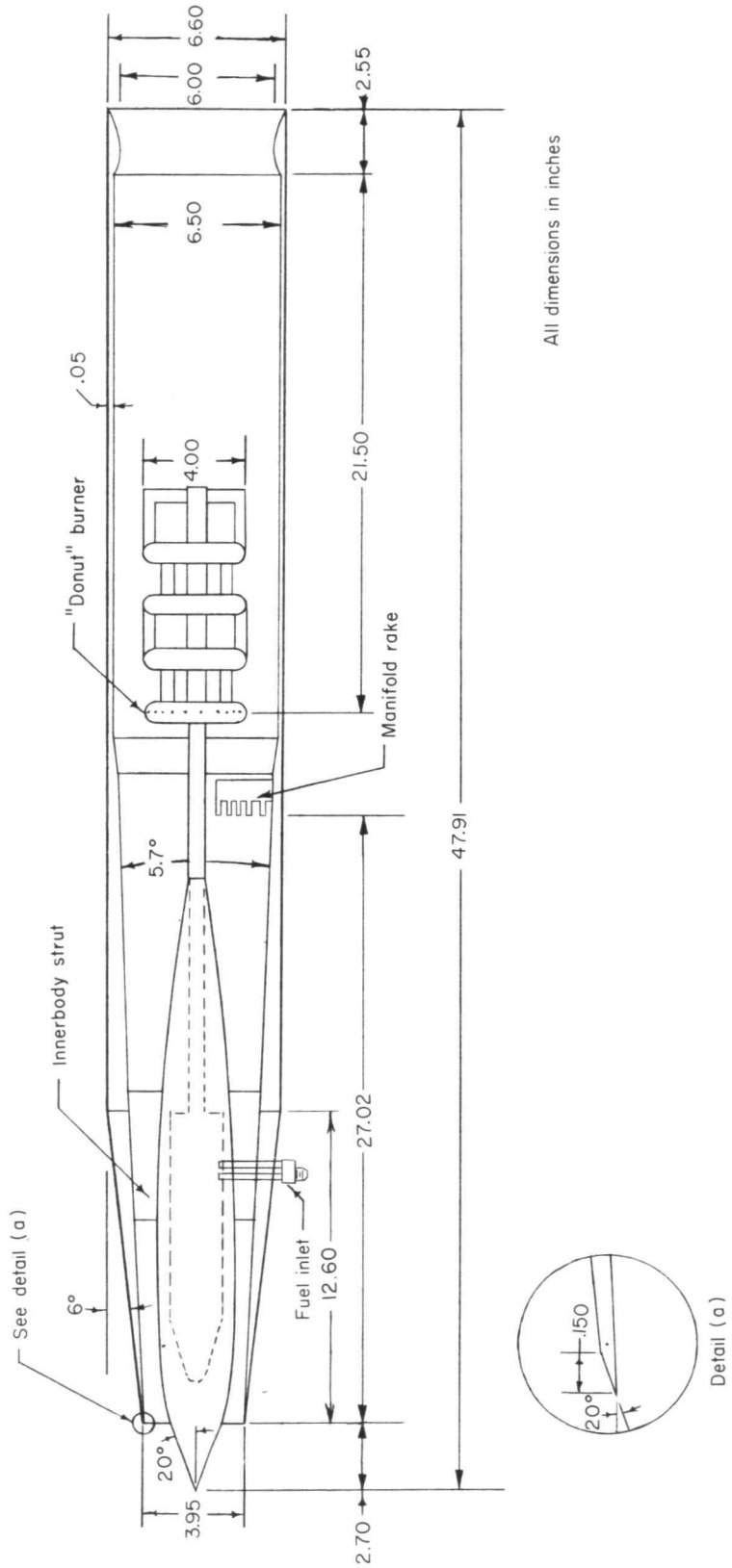
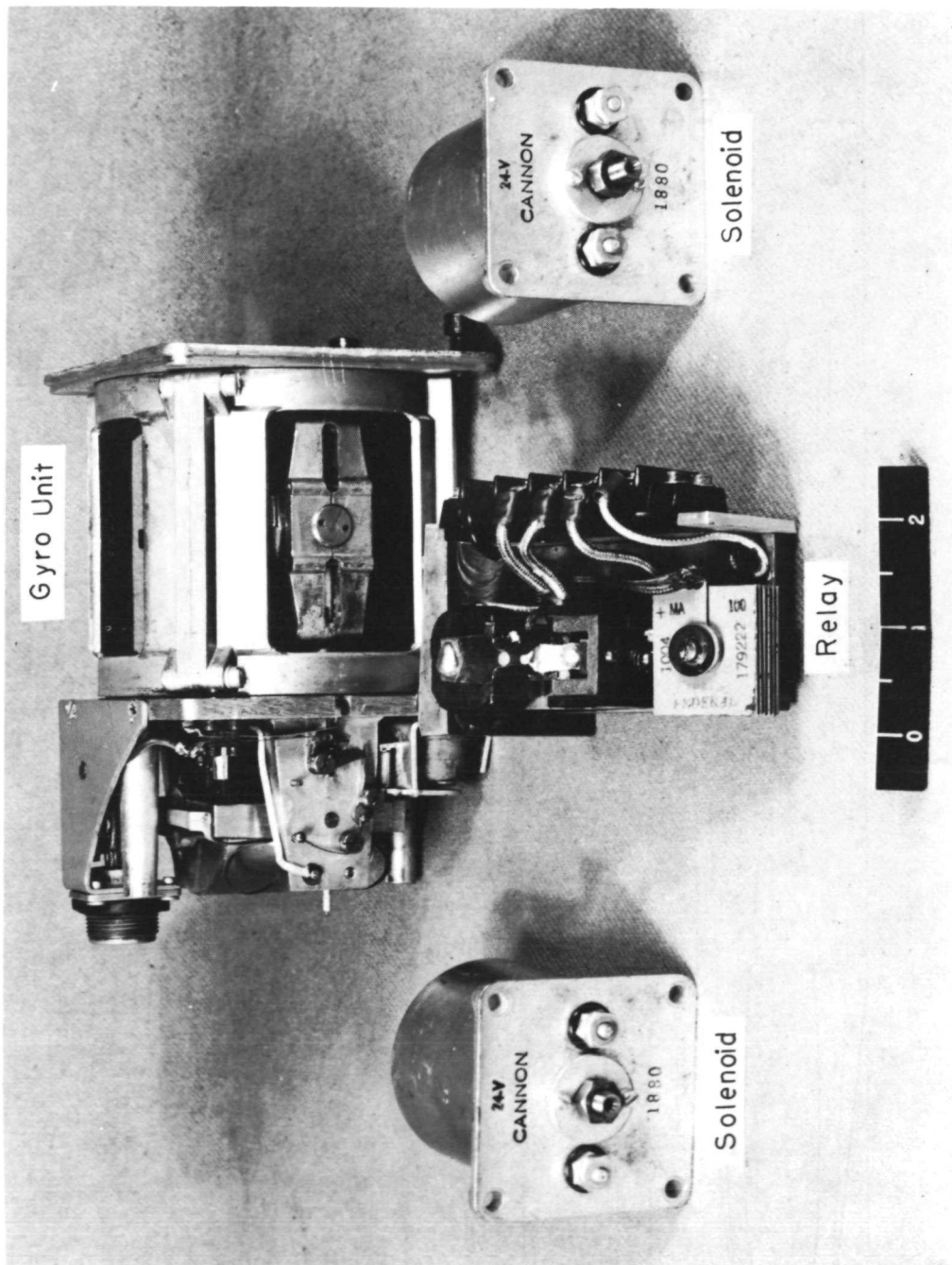
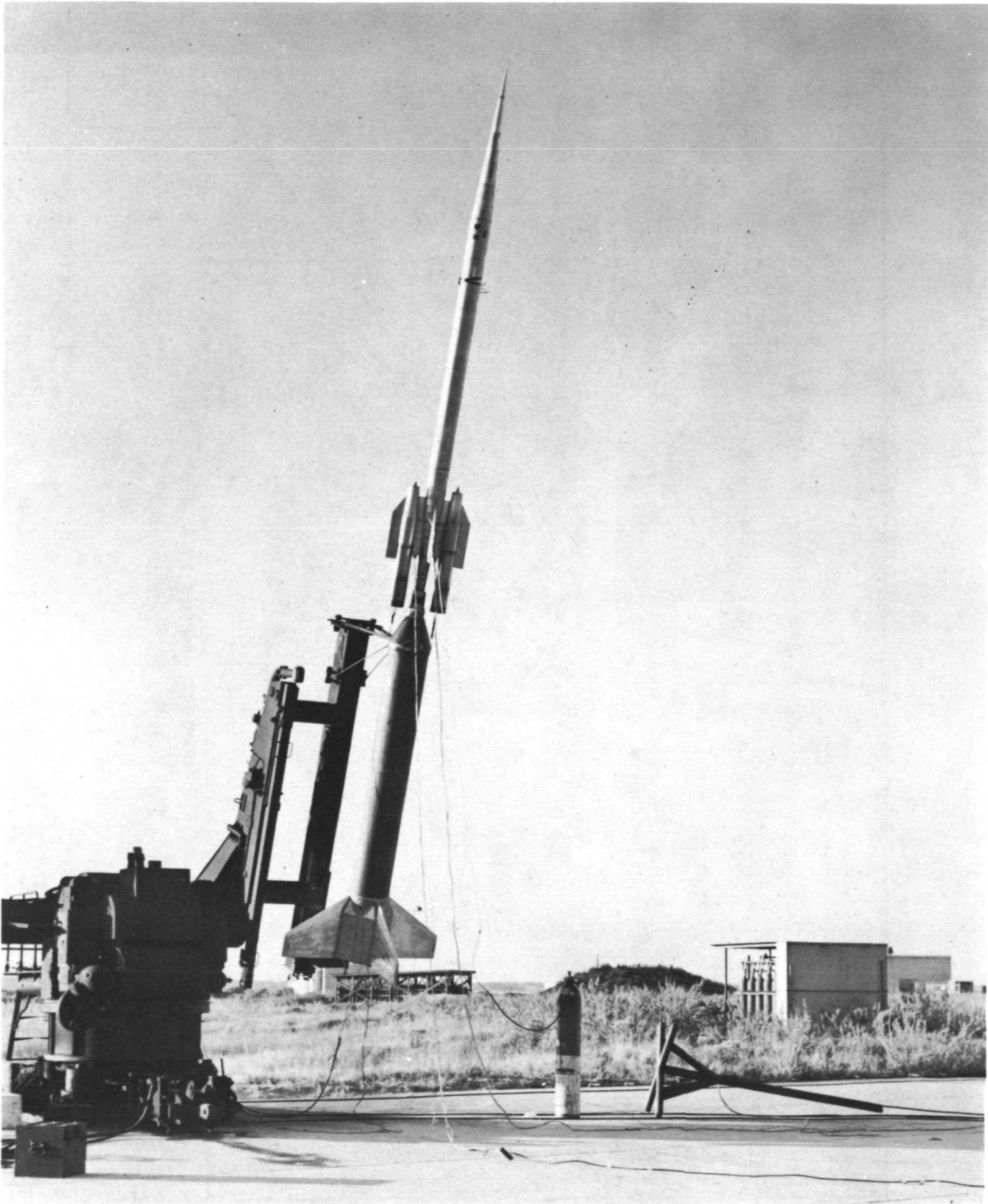


Figure 3.- Sketch of test vehicle ram-jet engine.

CONFIDENTIAL



L-85918.1
Figure 4.- Photograph of roll-stabilization system components.



L-86649

Figure 5.- Photograph of test vehicle and booster on the launcher.

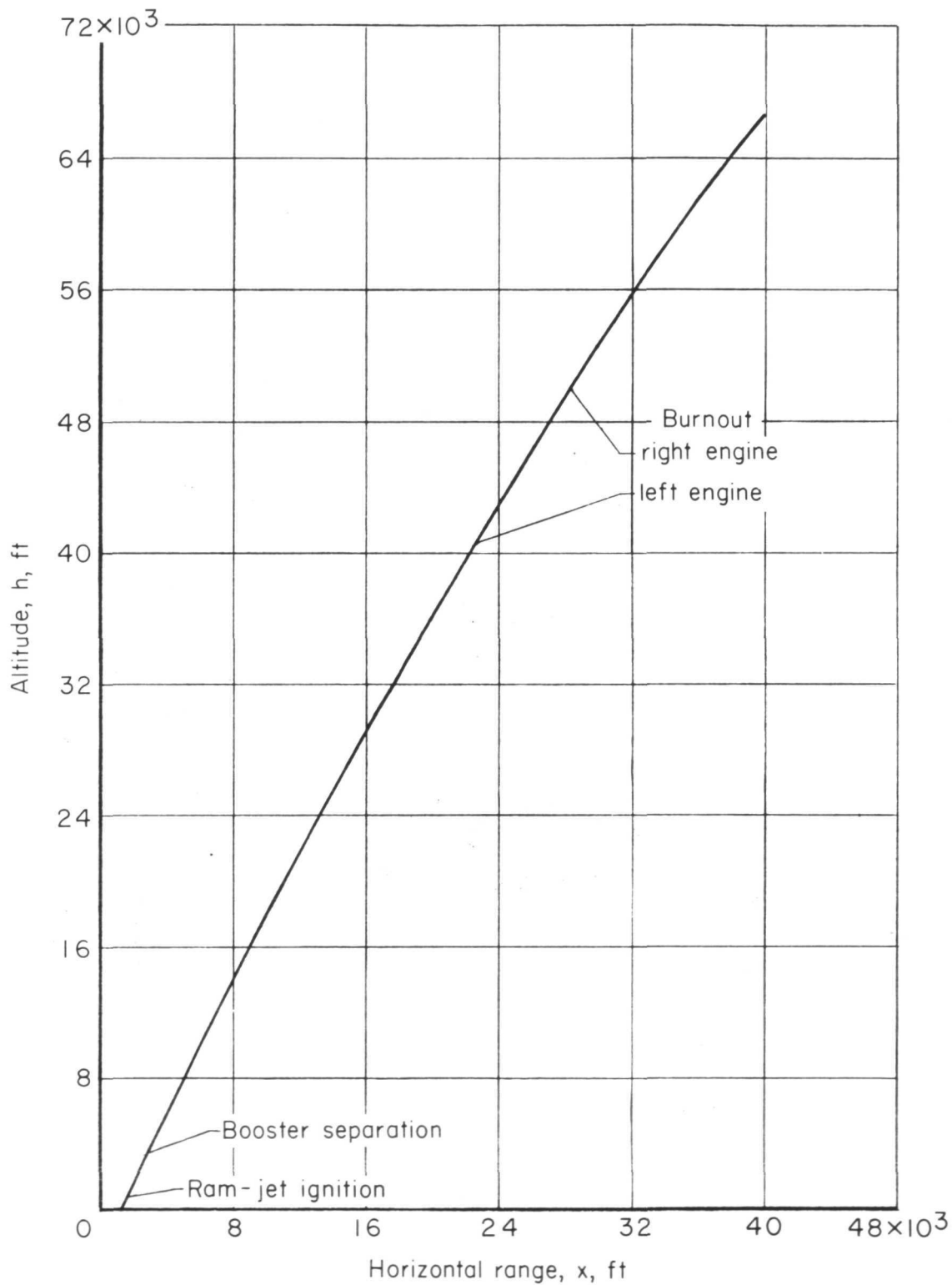


Figure 6.- Flight path of the test vehicle.

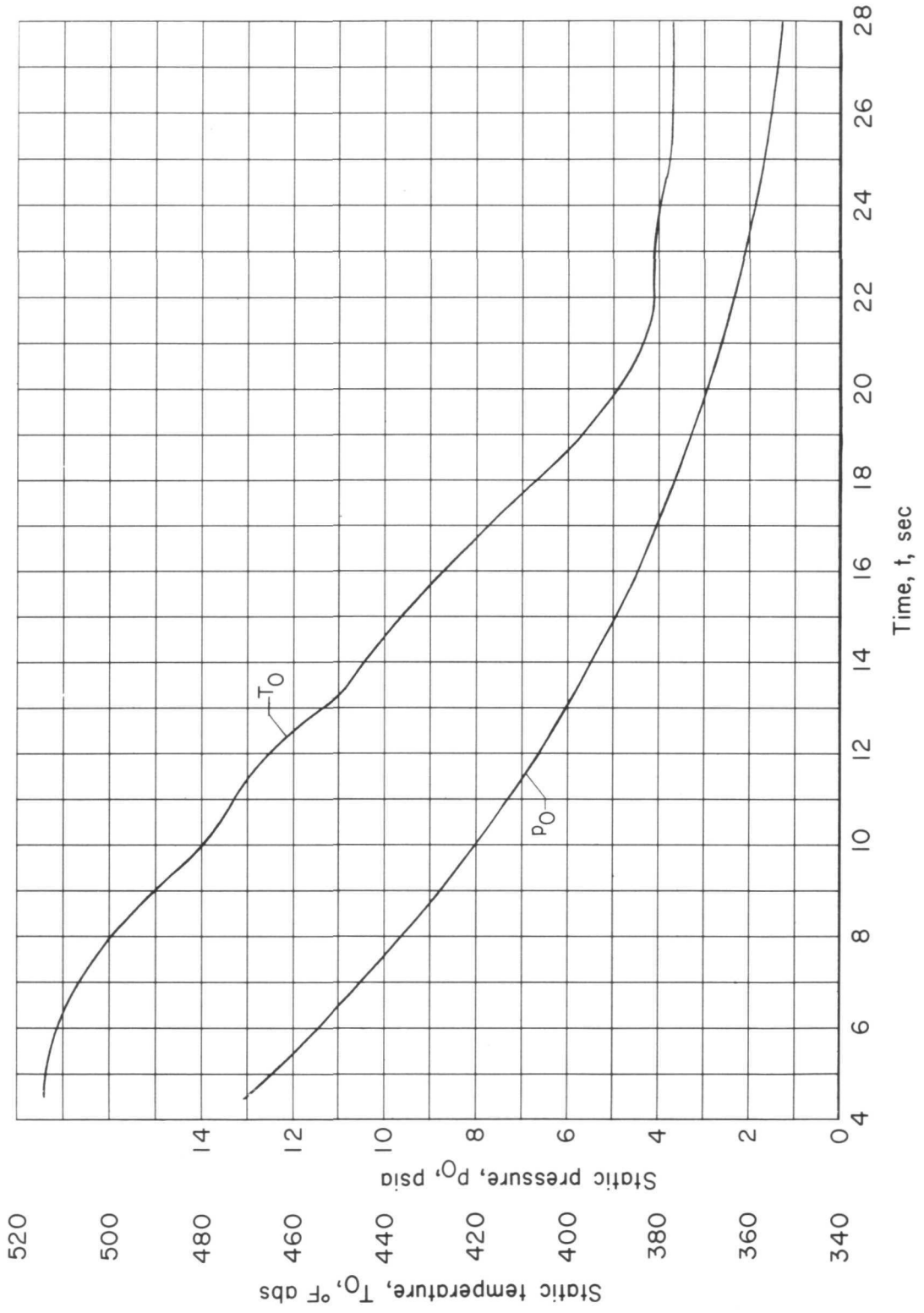


Figure 7.- Static temperature and pressure variation with time.

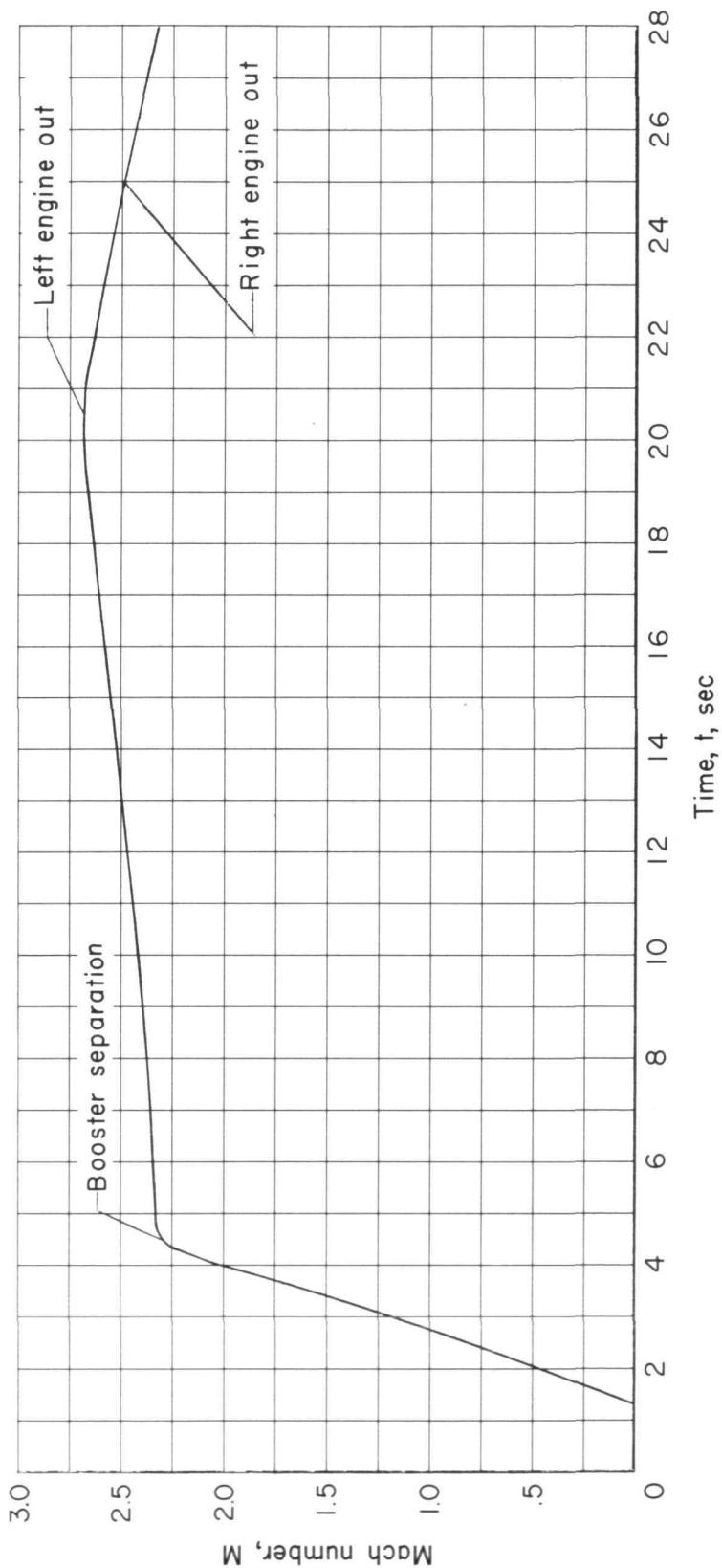


Figure 8.- Mach number time-history of the flight.

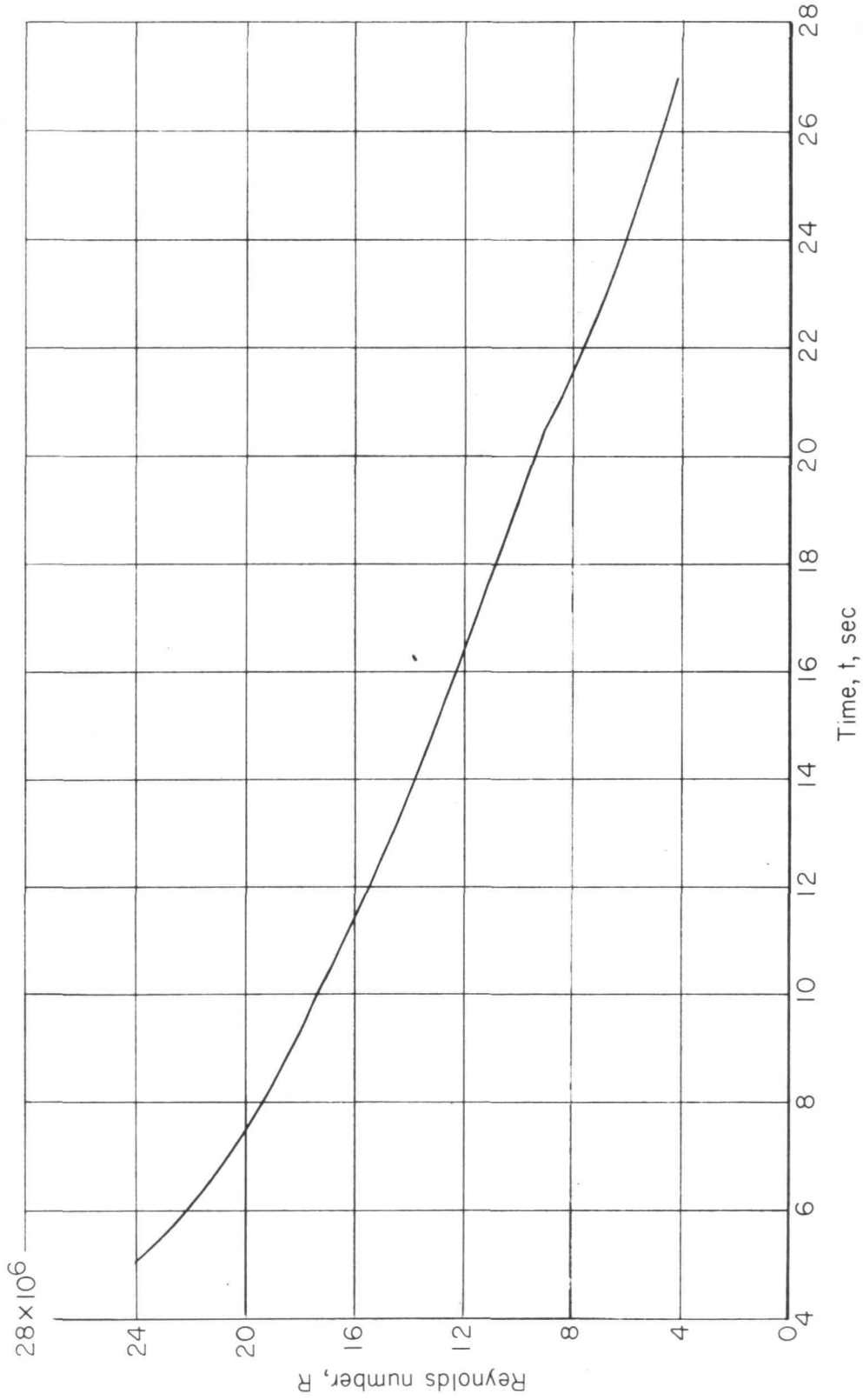


Figure 9.- Reynolds number variation with time (Reynolds number based on 1.67 ft mean chord of the delta fin).

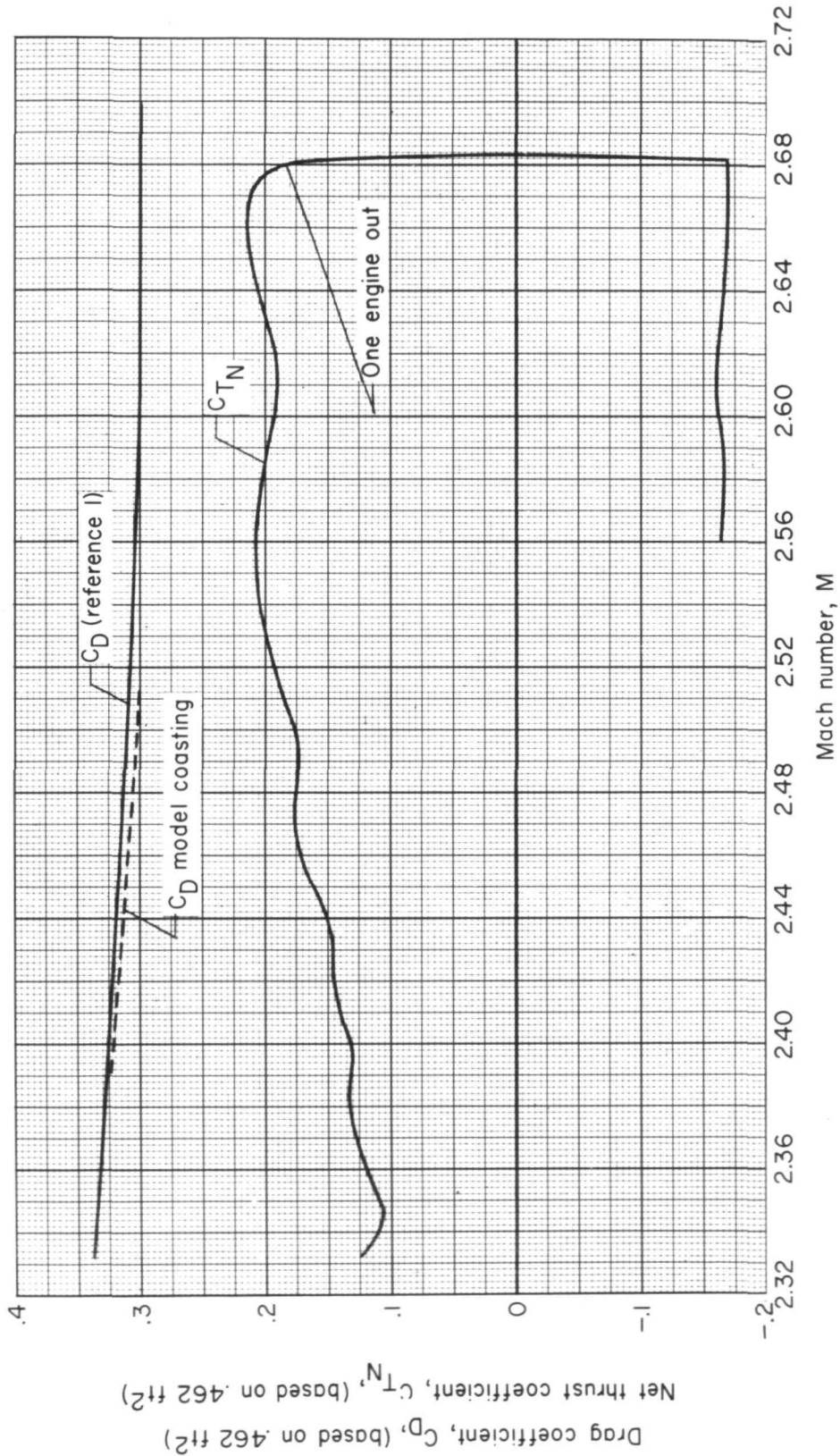


Figure 10.- Net thrust coefficient (thrust minus drag) and drag coefficient variation with Mach number.

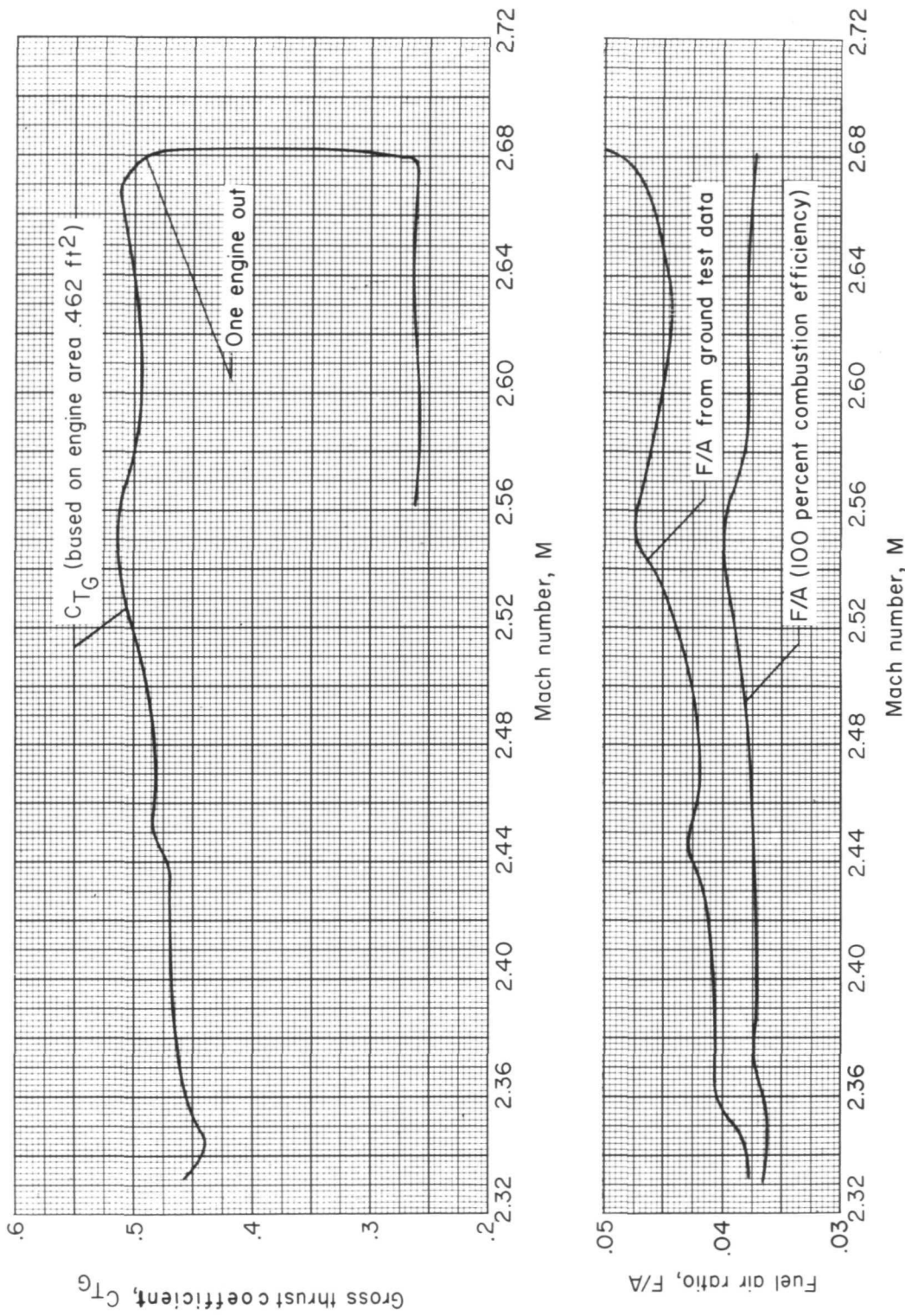


Figure 11.- Gross thrust coefficient and fuel air ratio variation with Mach number.

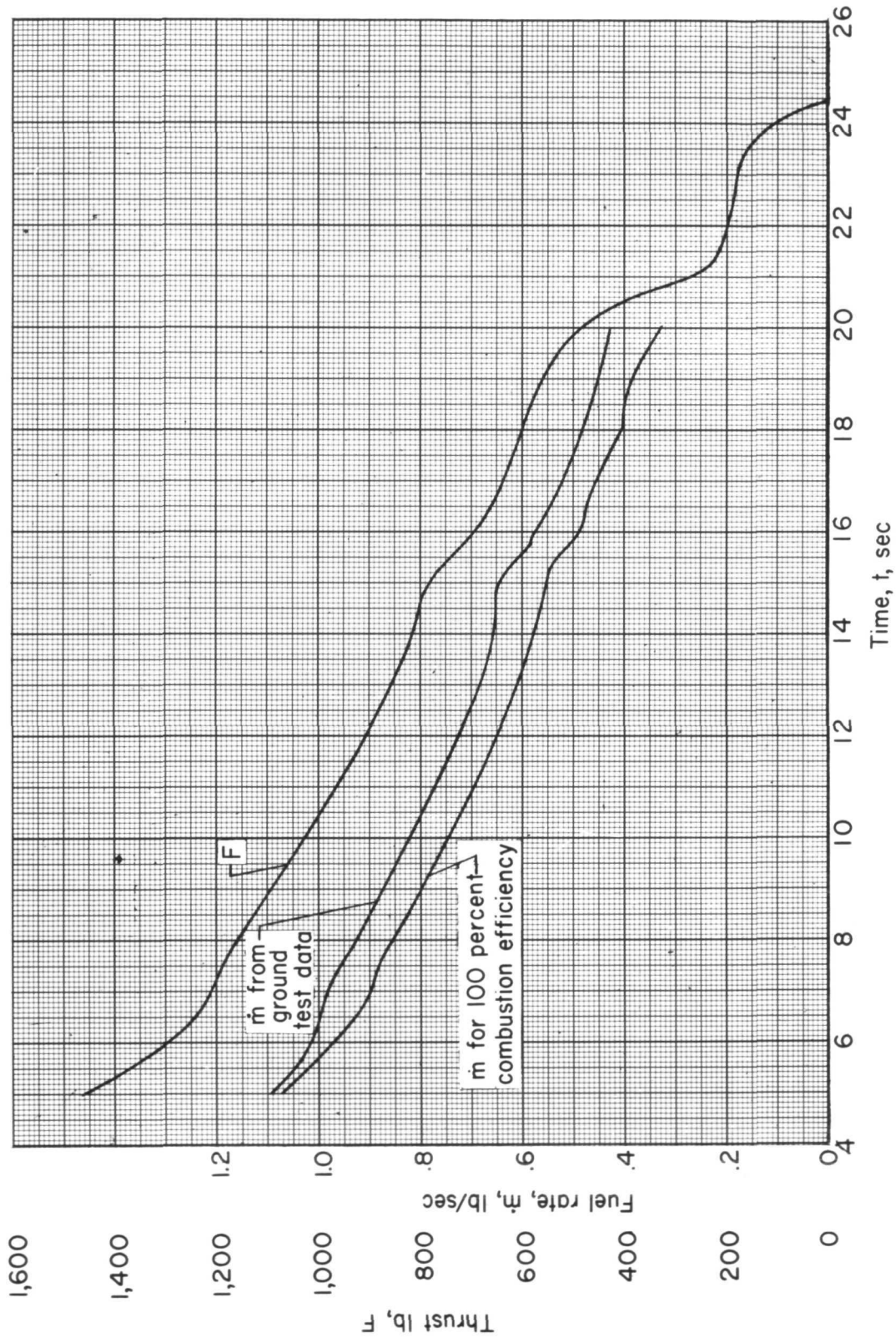


Figure 12.- Gross thrust and fuel rate variation with time.

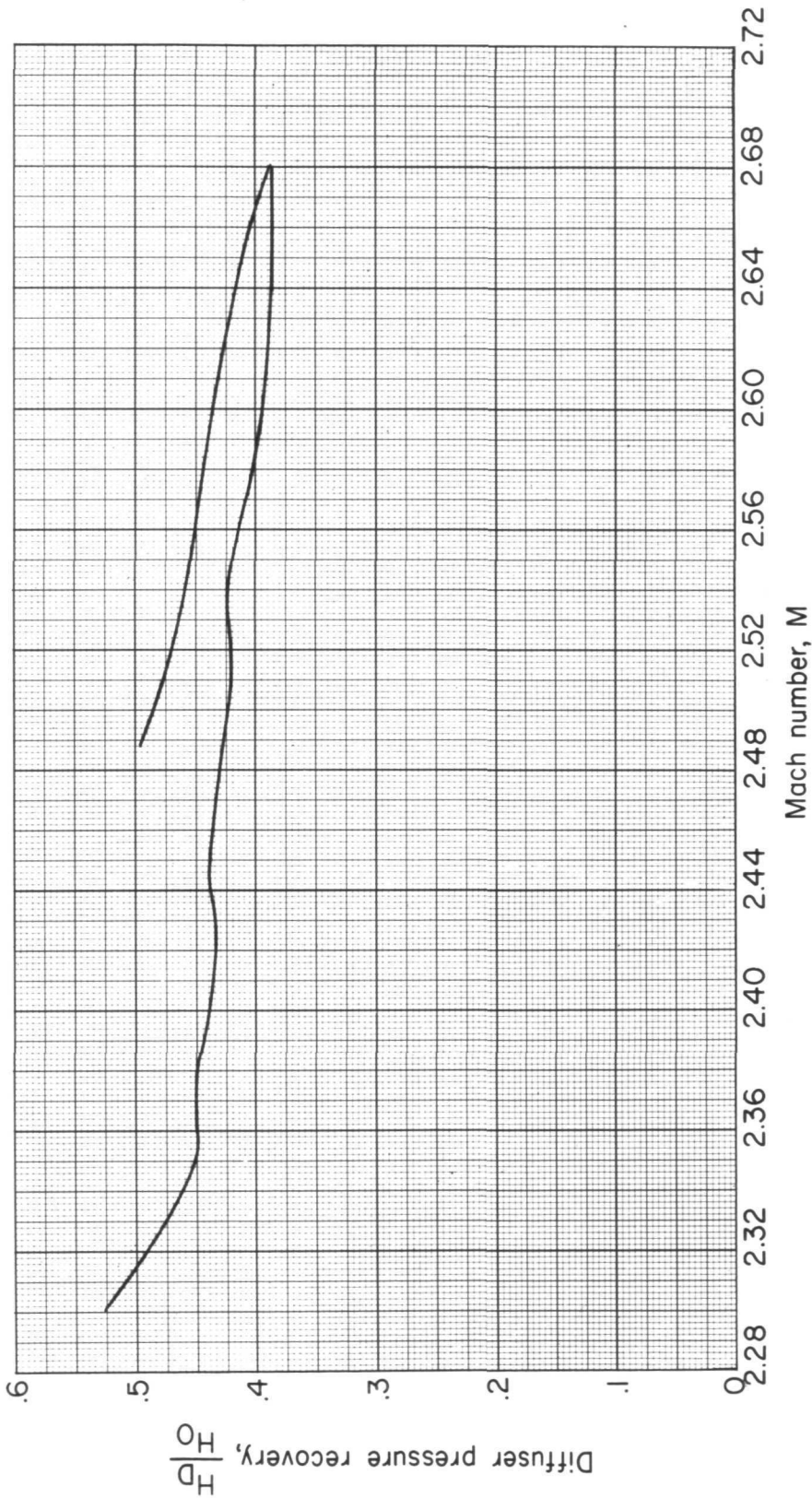


Figure 13.- Diffuser pressure recovery variation with Mach number.

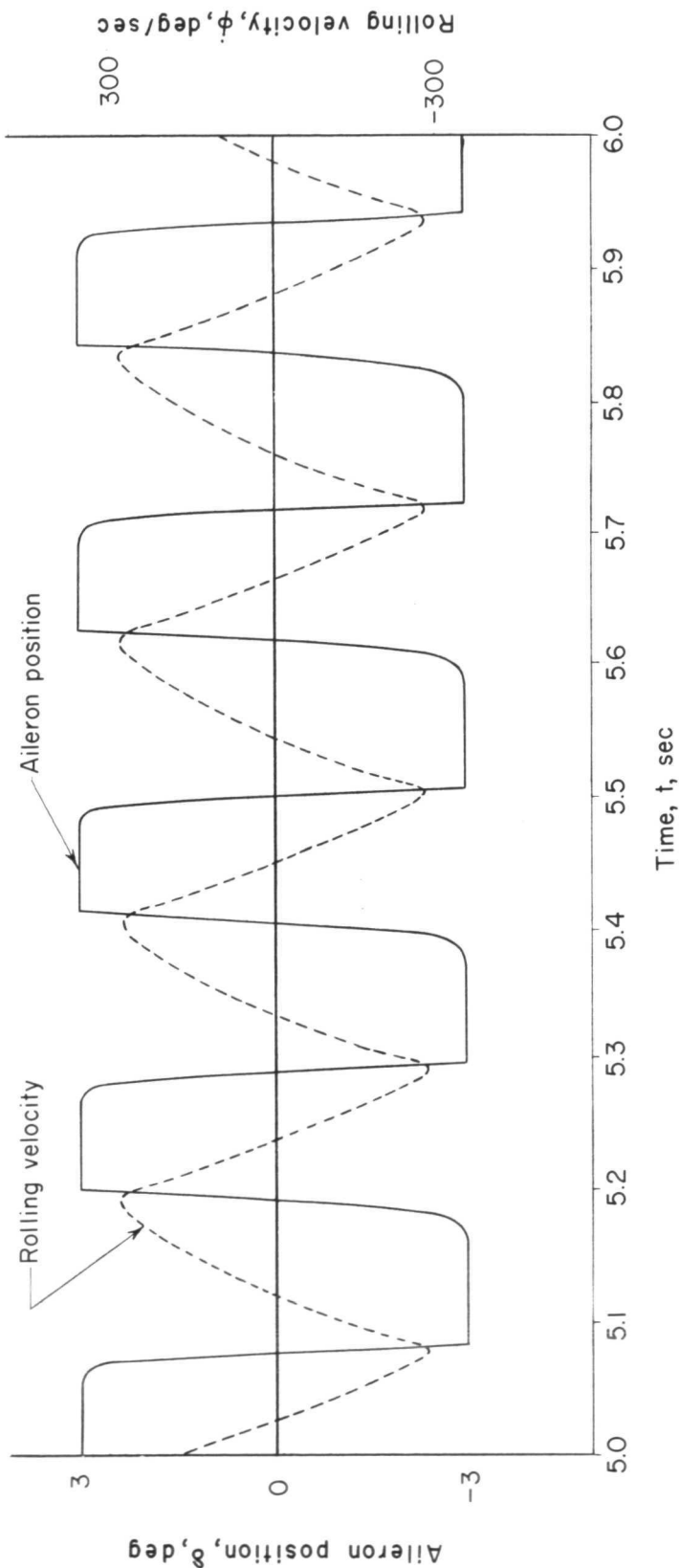


Figure 14.- Sample of the rolling velocity and aileron position as they appeared on the telemeter record.

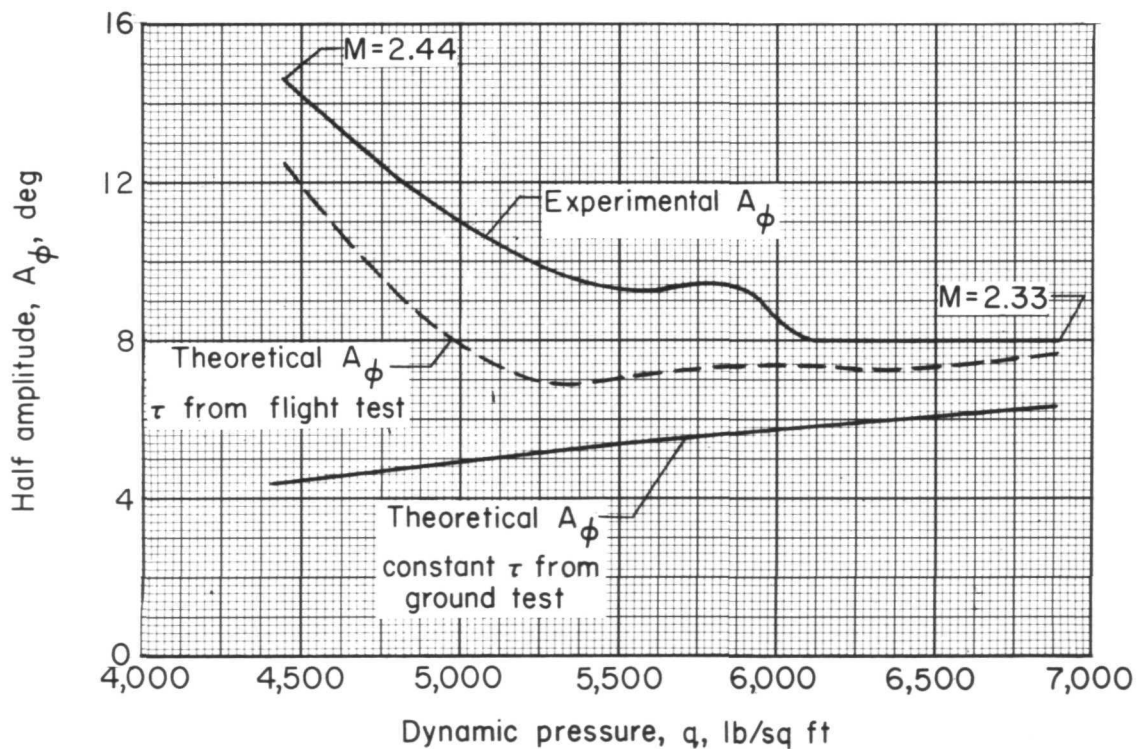
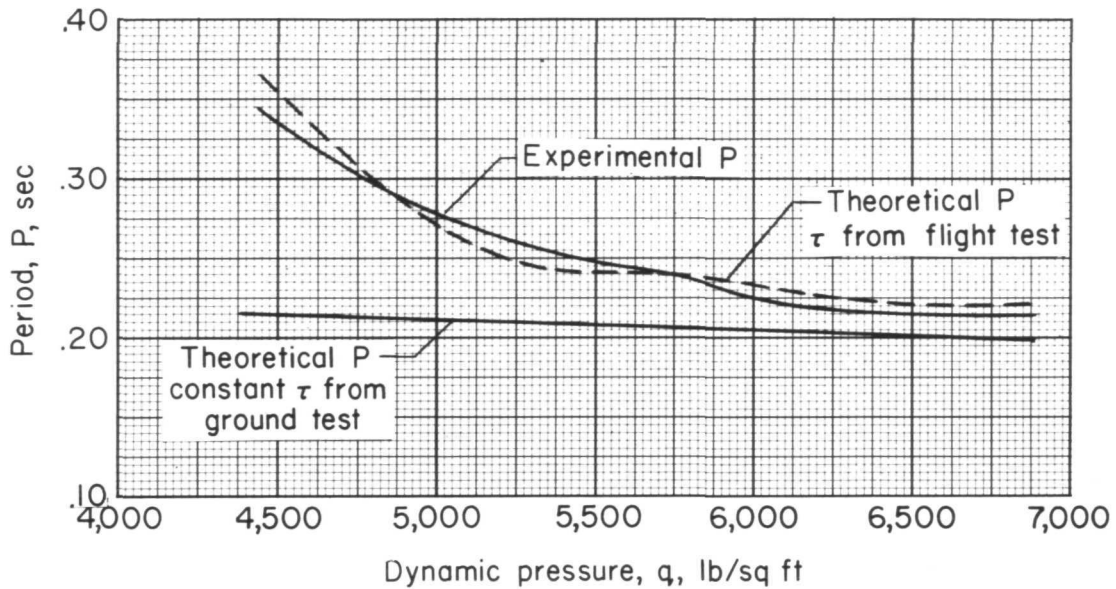


Figure 15.- Experimental and theoretical roll half amplitude and period as a function of time.

DECLASSIFIED